Excited-State Enantiomer Interconversion Kinetics Probed by Time-Resolved Chiroptical Luminescence Spectroscopy. The Solvent and Temperature Dependence of Λ-Eu(dpa)$_3^{3-}$ ⇄ Δ-Eu(dpa)$_3^{3-}$ Enantiomer Interconversion Rates in Solution†

Deborah P. Glover-Fischer,‡ David H. Metcalf,‡ Todd A. Hopkins,‡ Vincent J. Pugh,‡ Sarah J. Chisdes,‡ Jouko Kankare,§ and F. S. Richardson*,‡

Department of Chemistry, University of Virgnia, Charlottesville, Virginia 22901, and Department of Chemistry, University of Turku, FIN-20014 Turku, Finland

Received October 29, 1997

Trisdipicolinate coordination complexes of europium(III), Eu(dpa)$_3^{3-}$, have chiral, three-bladed propeller-like structures with either left-handed or right-handed structural helicity about a 3-fold symmetry axis. The left- and right-handed forms of these structures, labeled here as Λ and Δ, respectively, are structural enantiomers, and they exhibit characteristic circular dichroic absorption and emission properties in their optical excitation and luminescence spectra. In solution media that contain no other chiral species, the Eu(dpa)$_3^{3-}$ complexes exist as a racemic mixture of *interconverting* Λ and Δ enantiomeric structures (optical isomers). This racemic mixture of Λ- and Δ-Eu(dpa)$_3^{3-}$ complexes exhibits no chiroptical properties; but if it is excited with a pulse of circularly polarized light, partially resolved ground- and excited-state populations of Λ and Δ enantiomers are created, and these populations exhibit chiroptical properties reflective of their enantiomeric compositions (defined in terms of *enantiomeric excess* quantities). In this study, time-resolved chiroptical luminescence (TR-CL) measurements are used to monitor changes in excited-state enantiomeric excess as a function of time after circularly polarized excitation, and the rate parameters derived from these measurements are related to the rate constants of Λ ⇌ Δ processes. Measurements are performed over a range of sample temperatures, and the temperature-dependent rate data are analyzed in terms of Arrhenius and Eyring activation models. Results are reported for solution samples prepared in six different solvent media: H_2O, D_2O, an ethylene glycol−H_2O mixture, CH_3OH, C_2H_5-OH, and CH_3CN. These results show a significant solvent dependence both in the rates of Λ ⇌ Δ enantiomer interconversion processes and in the thermal activation energies determined for these processes.

Introduction

Several years ago we described a method for measuring enantiomer interconversion kinetics in solution samples that contain a racemic mixture of optical isomers.[1,2] The method is based on the use of circularly polarized light to prepare a nonracemic excited-state population of the optical isomers and the subsequent use of time-resolved chiroptical luminescence (TR-CL) measurements to follow changes in the enantiomeric composition of this population during its decay to ground state species. The enantiomeric excess generated in the initially prepared excited-state population (via circularly polarized optical excitation) depends on the *circular dichroic absorption* properties of the ground-state isomers, and detection of this enantiomeric excess and its evolution in time (via TR-CL measurements) depends on the *circular dichroic emission* properties of the excited-state isomers. The combined use of circularly polarized excitation and TR-CL measurements (hereafter referred to as CPEx/TR-CL spectroscopy) in studies of enantiomer interconversion kinetics is, of course, applicable only to luminescent molecular systems, and the information obtained from the measurements pertains in large part to dynamical processes that occur in the excited (emitting) states of the optically active systems. Furthermore, the time-development of the processes being probed must fall within the time window of the excited-to-ground-state decay processes in the systems.

In our first applications of CPEx/TR-CL spectroscopy as a probe of enantiomer interconversion kinetics we focused on excited-state racemization processes in H_2O and D_2O solution samples of Eu(dpa)$_3^{3-}$ and Eu(cda)$_3^{6-}$ (where dpa denotes a dipicolinate ligand and cda denotes a chelidamate ligand).[1,2] Each of these complexes has a chiral tristerdentate chelate structure of trigonal dihedral (D_3) symmetry, and in aqueous solution each exists as a racemic mixture of rapidly interconverting optical isomers (enantiomers). The isomers are generally labeled as Λ or Δ, indicating either *left-handed* (Λ) or *right-handed* (Δ) structural chirality (or helicity) about the 3-fold symmtery axis of the complex. The emitting state in these complexes is the lowest-energy $^5D_0$ multiplet level of Eu^{3+} ($4f^6$), which is located ca. 17 240 cm^{-1} above the $^7F_0$ (*ground*) multiplet level of Eu^{3+} ($4f^6$). At room temperature, the luminescence decay constants for Eu(dpa)$_3^{3-}$ and Eu(cda)$_3^{6-}$ are ca. 622 and 868 s^{-1}, respectively, in H_2O solutions, and ca. 313 and 445 s^{-1}, respectively, in D_2O solutions. These decay constants exhibit some temperature-dependent variations between 293 and 353 K, but over this temperature range the emitting populations of Eu(dpa)$_3^{3-}$ and Eu(cda)$_3^{6-}$ are sufficiently long-lived to permit TR-CL measurements of enanti-

* To whom correspondence should be addressed.
† dpa = dipicolinate dianion (2,6-pyridinedicarboxylate).
‡ Department of Chemistry, University of Virginia.
§ Department of Chemistry, University of Turku.

(1) Metcalf, D. H.; Snyder, S. W.; Demas, J. N.; Richardson, F. S. *J. Am. Chem. Soc.* **1990**, *112*, 469−479.
(2) Metcalf, D. H.; Snyder, S. W.; Demas, J. N.; Richardson, F. S. *J. Phys. Chem.* **1990**, *94*, 7143−7153.

S0020-1669(97)01370-0 CCC: $15.00
Published on Web 05/23/1998

omer interconversion kinetics to be made over time periods of up to 6 ms in duration (after a CPEx pulse has been applied to a sample). These periods of observation proved to be quite sufficient for characterizing $\Lambda \rightleftarrows \Delta$ interconversion rate processes that occur in the $^5D_0$ excited state of $Eu(dpa)_3^{3-}$ and $Eu(cda)_3^{6-}$ complexes in H_2O and D_2O solutions. The rates and mechanistic pathways of $\Lambda \rightleftharpoons \Delta$ processes in the equilibrium ground states of $Eu(dpa)_3^{3-}$ and $Eu(cda)_3^{6-}$ are expected to be essentially identical to those that occur in the $^5D_0$ excited state. This is due to the fact that the creation of $^5D_0$ from ground-state species involves only a one-electron excitation *within* the $4f^6$ electronic configuration of Eu^{3+} (i.e., an intraconfigurational 4f−4f transition), and it is well-known that the 4f electrons of lanthanide ions generally have a very weak influence on the coordination geometries and stereochemical dynamics of lanthanide complexes.

Among the most fascinating findings derived from our CPEx/TR-CL studies of $Eu(dpa)_3^{3-}$ and $Eu(cda)_3^{6-}$ were the differences observed between the enantiomer interconversion rate parameters determined for the complexes in H_2O versus D_2O solutions. The rate constants determined for the $\Lambda \rightleftharpoons \Delta$ processes in H_2O solutions were somewhat larger, but less temperature-dependent, than the rate constants determined for these processes in D_2O solutions. In each case, the temperature-dependent rate constant data yielded linear ln k_c vs $1/T$ plots (where k_c denotes the enantiomer interconversion rate constant) over the 293−353 K temperature range, and in each case the kinetics of the $\Lambda \rightleftharpoons \Delta$ processes were too slow to be measured accurately below 293 K.

In the present study, we reexamine the temperature dependence of Λ-$Eu(dpa)_3^{3-} \rightleftharpoons \Delta$-$Eu(dpa)_3^{3-}$ enantiomer interconversion kinetics in H_2O and D_2O solution samples, using new data obtained from improved CPEx/TR-CL measurement techniques. We also report results obtained from CPEx/TR-CL measurements performed on $Eu(dpa)_3^{3-}$ complexes in *nonaqueous* solution samples and in samples where the solvent is an ethylene glycol/water mixture. These results, combined with those obtained for $Eu(dpa)_3^{3-}$ in H_2O and D_2O solutions, yield further information about the solvent and temperature dependence of Λ-$Eu(dpa)_3^{3-} \rightleftharpoons \Delta$-$Eu(dpa)_3^{3-}$ processes in solution. This information is of considerable practical value in applications of $Eu(dpa)_3^{3-}$ complexes as luminescent probes of intermolecular chiral recognition processes in solution,[3,4] and it is also of some importance in developing a general understanding of how solvent molecules can mediate intramolecular structural transformations in solute species.

The mechanistic details of the structural transformations that occur in Λ-$Eu(dpa)_3^{3-} \rightleftharpoons \Delta$-$Eu(dpa)_3^{3-}$ processes in solution have, so far, eluded experimental characterization. However, it is reasonable to assume that on the time scale of our CPEx/TR-CL measurements the $Eu(dpa)_3^{3-}$ complexes remain constitutively intact and undergo $\Lambda \rightleftharpoons \Delta$ stereochemical transformations via an *intramolecular* mechanistic pathway.[1] To follow such a pathway, at least two of the three bicyclic chelate rings in the complexes must undergo concerted rotational motions (about their respective 2-fold symmetry axes) that carry the complexes from one enantiomeric form to the other via an *achiral* transition-state structure. These rotational motions of the chelate rings almost certainly require displacements and induce disturbances in the solvent structure around the complexes, and the size and shape of the solvent cavity required to accommodate the transition-state structures of the complexes are likely to be somewhat different from those needed to accommodate the equilibrium-state enantiomeric structures.

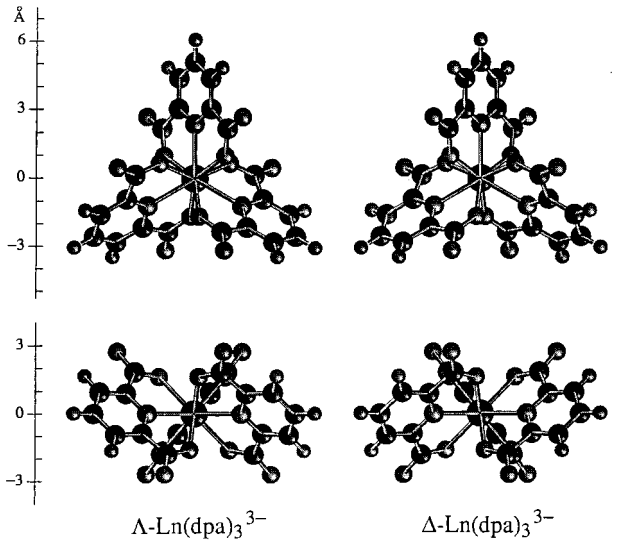

Figure 1. Structural representations of the Λ-$Eu(dpa)_3^{3-}$ and Δ-$Eu(dpa)_3^{3-}$ enantiomers as viewed along the trigonal symmetry axes (top structures) and along one of the digonal (C_2) symmetry axes (bottom structures).

The mechanistic considerations discussed above suggest that any structural elaborations of the chelate ring systems in the $Eu(dpa)_3^{3-}$ complexes might be expected to significantly alter the kinetics of the $\Lambda \rightleftharpoons \Delta$ enantiomer interconversion processes. To test this notion, we carried out a series of CPEx/TR-CL experiments on aqueous solutions of a complex in which a Eu^{3+} ion is coordinated (via tristerdentate chelation) to three 4-(phenylethynyl)-2,6-pyridinedicarboxylate ligands. These ligands, which may be alternatively named as 4-phenylethynyldipicolinates and given the abbreviation pe-dpa, differ from the dpa ligands of $Eu(dpa)_3^{3-}$ by the substitution of a Ph−C≡C− moiety for an H atom at the 4-position of the pyridine ring. The $Eu(pe\text{-}dpa)_3^{3-}$ complexes formed by these ligands have chelate-ring backbone structures identical to those in $Eu(dpa)_3^{3-}$, but each chelate ring system in $Eu(pe\text{-}dpa)_3^{3-}$ has a large Ph−C≡C− appendage that extends radially out to about 11 Å beyond the inner-coordination sphere of ligand donor atoms. These Ph−C≡C− appendages have a paddle-like shape, and their rotational motions in intramolecular Λ-$Eu(pe\text{-}dpa)_3^{3-} \rightleftharpoons \Delta$-$Eu(pe\text{-}dpa)_3^{3-}$ transformations would be expected to meet with considerable frictional resistance from solvent molecules. In fact, we find that the thermal activation energy for $\Lambda \rightleftharpoons \Delta$ processes in aqueous solutions of $Eu(pe\text{-}dpa)_3^{3-}$ is nearly 20 kJ/mol greater than that determined for these processes in aqueous solutions of $Eu(dpa)_3^{3-}$.

Structural drawings of the Λ and Δ enantiomers of $Eu(dpa)_3^{3-}$ are shown in Figure 1, and the structures of the dpa and pe-dpa ligands are compared in Figure 2.

Theory and Measurement Methodology

The basic theory underlying the use of CPEx/TR-CL spectroscopy in studies of excited-state enantiomer interconversion kinetics has been presented in some detail elsewhere,[1−3] and here we shall give only a brief review of those parts that are directly relevant to the present study. In CPEx/TR-CL spectroscopy, one excites a sample with a pulse of either left (l)- or

(3) Richardson, F. S.; Metcalf, D. H. in *Circular Dichroism: Principles and Applications;* Nakanishi, K., Berova, N., and Woody, R., Eds.; VCH Publishers: New York, 1994; Chapter 7, pp 153−177.
(4) Glover-Fischer, D. P.; Metcalf, D. H.; Bolender, J. P.; Richardson, F. S. *Chem. Phys.* **1995**, *198*, 207−234.

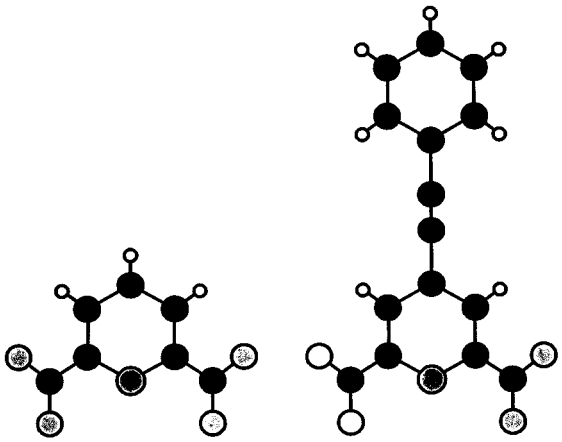

Figure 2. Comparison of the dipicolinate (dpa) and 4-phenylethylyl-dipicolinate (pe-dpa) ligand structures.

right (r)-circularly polarized light and then measures the relative intensities of left- and right-circularly polarized light in the sample luminescence as a function of time (after excitation). These polarization- and time-resolved luminescence intensities are then combined to obtain the following quantities:

$$I(\lambda',t) = I_l(\lambda',t) + I_r(\lambda',t) \tag{1}$$

$$\Delta I(\lambda',t) = I_l(\lambda',t) - I_r(\lambda',t) \tag{2}$$

$$g_{em}(\lambda',t) = \frac{2\Delta I(\lambda',t)}{I(\lambda',t)} \tag{3}$$

where $I_l(\lambda',t)$ and $I_r(\lambda',t)$ denote, respectively, the left- and right-circularly polarized luminescence intensities measured at time t (after excitation at $t \leq 0$) and at an emission wavelength λ'. The quantities I and ΔI are often referred to as *total luminescence* (TL) and *circularly polarized luminescence* (CPL) intensities, respectively, and g_{em} is commonly called an *emission dissymmetry factor*.

All of the data reported in this paper were obtained from CPEx/TR-CL measurements performed on solution samples that, prior to optical excitation, contain a racemic mixture of molecular enantiomers, which we denote here as Λ and Δ. Upon excitation with a pulse of either left- or right-circularly polarized light, one of the enantiomer populations in this mixture is preferentially excited over the other, and a *nonracemic* excited-state population of chiral luminophores (Λ^* and Δ^*) is created. The enantiomeric excess present in this excited-state population, *prior* to any molecular excited-state relaxation and decay processes, is given by

$$\eta_{ex}(\lambda,p) = \left(\frac{N_{ex}^{\Lambda^*} - N_{ex}^{\Delta^*}}{N_{ex}^{\Lambda^*} + N_{ex}^{\Delta^*}}\right)_{\lambda,p} \tag{4a}$$

$$= {}^1/_2 p g_{ab}^{\Lambda}(\lambda) = -{}^1/_2 p g_{ab}^{\Delta}(\lambda) \tag{4b}$$

where λ denotes excitation wavelength, p denotes the polarization state of the exciting radiation ($p = +1$ for left-circularly polarized light and -1 for right-circularly polarized light), $N_{ex}^{\Lambda^*}$ and $N_{ex}^{\Delta^*}$ are the concentrations of Λ^* and Δ^* created in the specified excitation process, and $g_{ab}^{\Lambda}(\lambda)$ and $g_{ab}^{\Delta}(\lambda)$ are *absorption dissymmetry factors* defined by

$$g_{ab}^{\Lambda}(\lambda) = 2\left(\frac{\epsilon_l^{\Lambda}(\lambda) - \epsilon_r^{\Lambda}(\lambda)}{\epsilon_l^{\Lambda}(\lambda) + \epsilon_r^{\Lambda}(\lambda)}\right) \tag{5}$$

$$g_{ab}^{\Delta}(\lambda) = 2\left(\frac{\epsilon_l^{\Lambda}(\lambda) - \epsilon_r^{\Lambda}(\lambda)}{\epsilon_l^{\Lambda}(\lambda) + \epsilon_r^{\Lambda}(\lambda)}\right) \tag{6}$$

where $\epsilon_l(\lambda)$ and $\epsilon_r(\lambda)$ denote molar absorption coefficients for left (l)- or right (r)-circularly polarized light of wavelength λ, and the superscripts Λ and Δ identify the relevant absorbing enantiomers.

For the systems of interest here, it may be assumed that the initially prepared excited-state population of luminophores relaxes to the relevant emitting-state population on a time scale too short for $\Lambda^* \rightleftharpoons \Delta^*$ processes to occur. Therefore, to a very good approximation, any changes in excited-state enantiomeric excess over time may be presumed to occur entirely within the emitting-state population of luminophores, and this time dependence of enantiomeric excess may be expressed as

$$\eta_{em}(t) = \left(\frac{N_{em}^{\Lambda^*}(t) - N_{em}^{\Delta^*}(t)}{N_{em}^{\Lambda^*}(t) + N_{em}^{\Delta^*}(t)}\right) = \frac{\Delta N_{em}(t)}{N_{em}(t)} \tag{7}$$

where $N_{em}^{\Lambda^*}(t)$ and $N_{em}^{\Delta^*}(t)$ denote the time-dependent concentrations of Λ^* and Δ^* in the emitting-state population of luminophores, and $\eta_{em}(0) = {}^1/_2 p g_{ab}^{\Lambda}(\lambda)$ from eq 4b.

The processes relevant to the decay kinetics of $N_{em}^{\Lambda^*}(t)$ and $N_{em}^{\Delta^*}(t)$ are

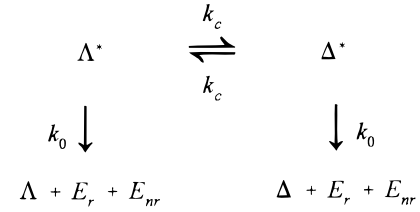

where k_c denotes the rate constant for enantiomer interconversion processes, k_0 is the rate constant for $\Lambda^* \rightarrow \Lambda$ and $\Delta^* \rightarrow \Delta$ decay processes, and E_r and E_{nr} denote radiative and nonradiative energies emitted in the latter processes. Given this kinetics scheme, the rate equations for $N_{em}^{\Lambda^*}(t)$ and $N_{em}^{\Delta^*}(t)$ decay are

$$-\frac{dN_{em}^{\Lambda^*}(t)}{dt} = (k_0 + k_c)\, N_{em}^{\Lambda^*}(t) - k_c N_{em}^{\Delta^*}(t) \tag{8}$$

$$-\frac{dN_{em}^{\Delta^*}(t)}{dt} = (k_0 + k_c)\, N_{em}^{\Delta^*}(t) - k_c N_{em}^{\Lambda^*}(t) \tag{9}$$

and the integrated rate expressions for the $N_{em}(t)$, $\Delta N_{em}(t)$, and $\eta_{em}(t)$ quantities of eq 7 are given by

$$N_{em}(t) = N_{em}(0)\exp[-k_0 t] \tag{10}$$

$$\Delta N_{em}(t) = N_{em}(0)\eta_{em}(0)\exp[-(k_0 + 2k_c)t] \tag{11}$$

$$\eta_{em}(t) = \eta_{em}(0)\exp[-2k_c t] \tag{12}$$

The time dependencies of the $I(\lambda',t)$, $\Delta I(\lambda',t)$, and $g_{em}(\lambda',t)$ quantities measured in our CPEx/TR-CL experiments (and defined by eqs 1−3) are determined by the time dependencies of $N_{em}(t)$, $\Delta N_{em}(t)$, and $\eta_{em}(t)$, respectively, and the data obtained from our TR-CL measurements are of the form

$$I(\lambda',t) = I(\lambda',0)\exp[-k_0 t] \quad (13)$$

$$\Delta I(\lambda',t) = \Delta I(\lambda',0)\exp[-(k_0 + 2k_c)t] \quad (14)$$

$$g_{em}(\lambda',t) = g_{em}(\lambda',0)\exp[-2k_c t] \quad (15)$$

The value of the $g_{em}(\lambda',0)$ factor in eq 15 is determined by the product $\eta_{em}(0)g_{em}^{\Lambda^*}(\lambda')$, where $g_{em}^{\Lambda^*}(\lambda')$ is the *intrinsic* emission dissymmetry factor of pure Λ^* enantiomers (at the emission wavelength λ'). If we assume, as previously discussed, that $\eta_{em}(0) = {}^1/_2 p g_{ab}^{\Lambda}(\lambda')$, then eq 15 may be reexpressed as

$$\begin{aligned} g_{em}(\lambda',t) &= g_{em}^{\Lambda^*}(\lambda')\eta_{em}(t) \\ &= g_{em}^{\Lambda^*}(\lambda')\eta_{em}(0)\exp[-2k_c t] \\ &= {}^1/_2 p g_{ab}^{\Lambda}(\lambda) g_{em}^{\Lambda^*}(\lambda')\exp[-2k_c t] \end{aligned} \quad (16)$$

where $p = \pm 1$, reflecting the use of either left- or right-circularly polarized excitation (at wavelength λ).

Measurements of $g_{em}(\lambda',t)$ provide a direct means for determining the enantiomer interconversion rate constant k_c. However, the feasibility of such measurements depends on the magnitude of the preexponential factor, $g_{ab}^{\Lambda}(\lambda)g_{em}^{\Lambda^*}$, in eq 16. The larger the magnitude of this factor is, the easier it is to make reliable measurements of $g_{em}(\lambda',t)$. Therefore, it is important to choose excitation and emission wavelengths in transition regions where $|g_{ab}^{\Lambda}|$ and $|g_{em}^{\Lambda^*}|$ are large. For the europium complexes examined in this study, the optimal choices for excitation wavelength (λ) are in the ${}^7F_0 \rightarrow {}^5D_1$ transition region of $Eu^{3+}(4f^6)$, which falls within the 526−528 nm excitation wavelength range, and the optimal choices for emission wavelength (λ') are in the ${}^7F_1 \leftarrow {}^5D_0$ transition region of $Eu^{3+}(4f^6)$, which falls within the 592−596 nm emission wavelength range. Working within these excitation and emission regions of $Eu^{3+}(4f^6)$ in $Eu(dpa)_3^{3-}$ complexes, one can find combinations of λ and λ' that yield $|g_{ab}^{\Lambda}||g_{em}^{\Lambda^*}|$ as large as 0.17.

Experimental Section

Preparation of H_2O, D_2O, and Ethylene Glycol/H_2O Solution Samples. A stock solution of $Eu(dpa)_3^{3-}$ in H_2O was prepared by the reaction of $Eu_2(CO_3)_3$ with 6 equivalents of dipicolinic acid and 3 equiv of Na_2CO_3 in H_2O. The resulting solution was heated mildly to drive off excess CO_2 and was then brought to pH 7 by dropwise addition of 1 M Na_2CO_3. The final solution was diluted with H_2O to bring the concentration to 50 mM $Eu(dpa)_3^{3-}$. A portion of this solution was then used to form a stock solution of $Eu(dpa)_3^{3-}$ in D_2O by first evaporating the H_2O under high vacuum, and then dissolving the resulting solid in an appropriate amount of D_2O to reach a final concentration of 20 mM $Eu(dpa)_3^{3-}$. The D_2O solution was stored in a vacuum desiccator until needed for the spectroscopic experiments. Another portion of the $Eu(dpa)_3^{3-}$/H_2O stock solution was mixed with ethylene glycol (EG) to form a sample in which the H_2O−EG solvent mixture contained 60% EG (by weight) and the concentration of $Eu(dpa)_3^{3-}$ was 10 mM.

Solution samples of $Eu(pe\text{-}dpa)_3^{3-}$ in H_2O were prepared following procedures identical to those described above for $Eu(dpa)_3^{3-}$ in H_2O, *except* that 4-phenylethynyldipicolinic acid was substituted for dipicolinic acid in the initial reaction mixture. The 4-phenylethynyldipicolinic acid was prepared by basic hydrolysis of the corresponding diethyl ester of this compound (with KOH in ethanol and subsequent acidification). The diethyl ester was synthesized according to methods described previously by Takalo and Kankare.[5]

Preparation of Nonaqueous Solution Samples. The sodium salts of $Eu(dpa)_3^{3-}$ complexes have very low solubilities in the nonaqueous solvents used in this study: CH_3OH, C_2H_5OH, and CH_3CN. However, the tetra-*n*-butylammonium (NBu_4^+) salts of $Eu(dpa)_3^{3-}$ are considerably more soluble in these solvents, and they can be used to prepare solution samples with the desired 1−10 mM concentration of $Eu(dpa)_3^{3-}$. All of the nonaqueous solution samples used in this study were prepared by dissolving $(NBu_4)_3[Eu(dpa)_3]$ directly in the solvent of interest. The preparation of $(NBu_4)_3[Eu(dpa)_3]$ was carried out by reaction of 1 equiv of Eu_2O_3 with 6 equiv of $dpaH_2$ in water and subsequent neutralization of the solution with 6 equiv of NBu_4HCO_3. The water was stripped off under vacuum, and the resulting solid was dried in a vacuum desiccator. The NBu_4HCO_3 was prepared by reaction of NBu_4OH with CO_2 in H_2O. A different synthesis for tetraalkylammonium salts of $Eu(dpa)_3^{3-}$ has been reported by Brayshaw et al.[6]

Spectroscopic Instrumentation and Measurements. The instrumentation for detection of time-resolved chiroptical luminescence has been described in several previous papers.[1,2] The solution sample in its fluorescence cuvette is held in a thermostated temperature-control block with a NIST traceable temperature sensor (Fischer Scientific) mounted in close proximity to the sample. The excitation (at 526.3 nm) is provided by either a pulsed N_2 laser (PRA LN1000) pumping a dye laser (PRA LN107) using Coumarin 540A as lasing dye or a Quantel Nd:YAG laser (YG660) pumping a Quantel dye laser (TDL60) using Coumarin 500 as the lasing dye. The excitation pulse is passed through a polarizer and a Fresnel rhomb to render it circularly polarized, and then through the bottom of the fluorescence cuvette. The emission is detected at 90° with respect to the excitation direction and passes through a photoelastic modulator (Hinds International PEM-80)−polarizer combination for analysis of the circularly polarized content of the emitted radiation. The emission is subsequently dispersed with a scanning Spex 0.75 m double-grating monochromator to allow for emission wavelength analysis/selection. The emission intensity is detected using a photon-counting photomultiplier tube (RCA C31034). The temporal and polarization characteristics of the emission are ascertained by correlating photon arrival times with time after the excitation pulse *and* the photoelastic modulator polarization state using gated photon-counting electronics.

Data Analysis. The kinetic parameters associated with excited-state emission decay processes and excited-state enantiomer interconversion processes are determined by fitting the experimental data ($I(\lambda',t)$, $\Delta I(\lambda',t)$, and $g_{em}(\lambda',t)$) to eqs 13−15. An adjustable correction for dark counts has to be included, and the actual equations used in the fitting are

$$I(\lambda',t) = I(\lambda',0)\exp[-k_0 t] + dc \quad (17)$$

$$\Delta I(\lambda',t) = \Delta I(\lambda',0)\exp[-(k_0 + 2k_c)t] \quad (18)$$

$$g_{em}(\lambda',t) = g_{em}(\lambda',0)\exp[-2k_c t] \times \frac{I(\lambda',t) - dc}{I(\lambda',t)} \quad (19)$$

Here, *dc* denotes the dark count term (which does not appear

(5) Takalo, H.; Kankare, J. *Acta Chem. Scand. B* **1987**, *41*, 219−221.
(6) Brayshaw, P. A.; Bünzli, J.-C. G.; Froidevaux, P.; Harrowfield, J. M.; Kim, Y.; Sobolev, A. N. *Inorg. Chem.* **1995**, *34*, 2068−2076.

in the $\Delta I(\lambda',t)$ expression). We use a Levenburg−Marquardt weighted nonlinear least-squares fitting technique, as implemented by Press et al.,[7] to determine the appropriate adjustable parameters ($I(\lambda',0)$, $\Delta I(\lambda',0)$, $g_{em}(\lambda',0)$, k_0, k_c, and/or dc) in the above expressions.

Thermal activation parameters for the enantiomer interconversion kinetics are derived by fitting temperature-dependent k_c data to the following linear expressions:

$$\ln k_c = \ln A - \frac{E_a}{RT} \text{ (Arrhenius)} \tag{20}$$

$$\ln\left(\frac{k_c}{T}\right) = \ln\left(\frac{k_B}{h}\right) + \frac{\Delta S^{\ddagger}}{R} - \frac{\Delta H^{\ddagger}}{RT} \text{ (Eyring)} \tag{21}$$

Here, k_B is Boltzmann's constant, h is Planck's constant, and R is the gas constant.

Results

General. All of the luminescence intensity spectra recorded for $Eu(dpa)_3^{3-}$ in the various solution samples exhibit essentially identical spectral dispersion characteristics, and in all cases these spectra show line (or band) structures diagnostic of $Eu(dpa)_3^{3-}$ complexes with trigonal-dihedral (D_3) symmetry. This applies to both the $I(\lambda') = I_l(\lambda') + I_r(\lambda')$ and $\Delta I(\lambda') = I_l(\lambda') - I_r(\lambda')$ spectra excited with circularly polarized light, and it indicates the lack of any strong solvent-dependent effects on the equilibrium structures of $Eu(dpa)_3^{3-}$. However, solvent effects are observed quite prominently in the luminescence lifetime data obtained for $Eu(dpa)_3^{3-}$ in the various solution samples, which implies that solvent molecules can play an active role in modulating the decay kinetics of the $^5D_0$ (Eu^{3+}) emitting level. The decay of $^5D_0$ (Eu^{3+}) in $Eu(dpa)_3^{3-}$ occurs predominantly via *nonradiative* processes, and it is generally believed that solvent molecules can contribute to these processes via multiphonon (solvent molecule)/4f electron (Eu^{3+}) coupling mechanisms.

The luminescence intensity spectra recorded for $Eu(pe\text{-}dpa)_3^{3-}$ complexes in H_2O solution samples are essentially identical to those recorded for $Eu(dpa)_3^{3-}$ complexes in H_2O. However, the luminescence lifetimes measured for $Eu(pe\text{-}dpa)_3^{3-}$ over the 20−80 °C temperature range are somewhat shorter than those measured for $Eu(dpa)_3^{3-}$ in H_2O over this same temperature range.

Examples of $I(\lambda')$ and $\Delta I(\lambda')$ spectra obtained for $Eu(dpa)_3^{3-}$ complexes in solution samples excited with circularly polarized light can be found in refs 1 and 3, and they will not be shown again here. In the following sections, we will focus on the results obtained from our time-resolved measurements of $I(\lambda',t)$ and $\Delta I(\lambda',t)$ in CPEx/TR-CL experiments where λ' was fixed at a value chosen to give large $|\Delta I|/I$ ratios. Included among those results are rate constants for enantiomer interconversion (k_c) and emitting-state decay (k_0) processes. The *luminescence lifetimes* alluded to in the preceding two paragraphs correspond to values of $1/k_0$.

$Eu(dpa)_3^{3-}$ in H_2O, D_2O, and H_2O−EG Solutions. Time-resolved $I = I_l + I_r$ and $\Delta I = I_l - I_r$ intensity data are shown in Figures 3−5 for $Eu(dpa)_3^{3-}$ in H_2O, D_2O, and H_2O−EG solution samples. Data acquired at nine different sample temperatures between 20 and 80 °C are shown. All of the data shown in these figures were obtained from CPEx/TR-CL experiments in which excitation was with *left*-circularly polarized light of wavelength 526.3 nm and emission detection was at 594.8 nm. An example of a g_{em} versus time plot is given in Figure 6. Recall that in our experiments, the time decay of g_{em} follows the time-decay of enantiomeric excess in the emitting-state population of luminophores, according to eq 16. At sample temperatures <20 °C, the observed g_{em} values remain essentially constant over the luminescence decay period, indicating enantiomer interconversion rates too slow to be detected on the time scale of our CPEx/TR-CL measurements.

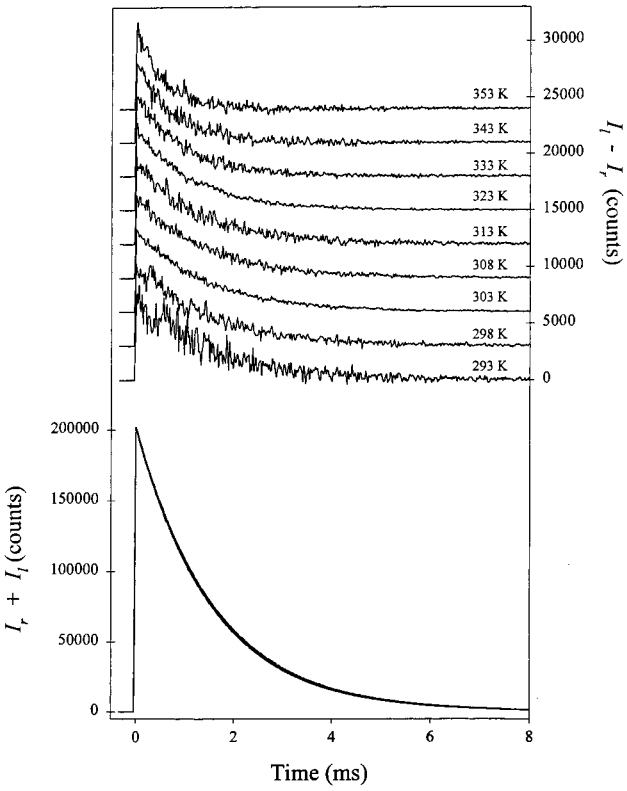

Figure 3. Time-resolved CPL (top noisy traces, $I_l - I_r$) and TL (bottom smooth traces, $I_l + I_r$) data obtained for 10 mM $Eu(dpa)_3^{3-}$ in H_2O at nine different sample temperatures. Excitation was with left-circularly polarized light at 526.3 nm, and emission intensities were measured at 594.8 nm. All the TL decay curves are overlaid, whereas the CPL decay curves are offset from one another by 3000 counts on the CPL axis.

In Table 1, we list the values of the k_0 and k_c rate constants determined from analyses of the $I(\lambda',t)$, $\Delta I(\lambda',t)$, and $g_{em}(\lambda',t)$ data obtained for $Eu(dpa)_3^{3-}$ in H_2O, D_2O, and H_2O−EG solution samples. Fits of the temperature-dependent k_c results to Arrhenius and Eyring equations (see eqs 20 and 21 given in an earlier section) yielded the thermal activation parameters listed in Table 2.

$Eu(pe\text{-}dpa)_3^{3-}$ in H_2O. In the CPEx/TR-CL experiments performed on $Eu(pe\text{-}dpa)_3^{3-}$ complexes in H_2O solution samples, excitation was with circularly polarized light of wavelength 526.1 nm, and emission detection was at 594.8 nm. The k_0 and k_c rate constants determined from the data obtained in these experiments are given in Table 3, and the thermal activation parameters derived from the Arrhenius and Eyring analyses of the temperature-dependent k_c results are shown in Table 2. Note the somewhat larger luminescence decay constants (k_0) determined for $Eu(pe\text{-}dpa)_3^{3-}$ versus $Eu(dpa)_3^{3-}$ complexes in H_2O, and note also the larger thermal activation energy parameters (E_a and $\Delta H^{\ddagger}$) determined for $\Lambda^* \rightleftharpoons \Delta^*$ processes in $Eu(pe\text{-}dpa)_3^{3-}$ versus $Eu(dpa)_3^{3-}$. Due to the comparatively faster luminescence decay kinetics of $Eu(pe\text{-}dpa)_3^{3-}$, the time-windows

(7) Press: W. H.; Flannery, B. P.; Teukolsky, S. A.; Vetterling, W. T. *Numerical Recipes in Pascal*; Cambridge University Press: Cambridge, UK, 1989; Chapter 14, pp 547−598.

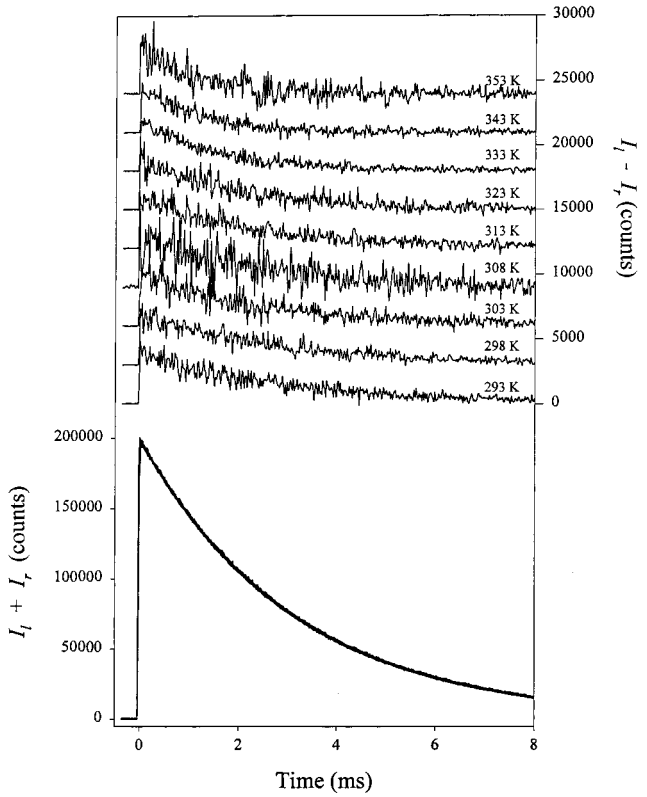

Figure 4. Time-resolved CPL (top noisy traces, $I_l - I_r$) and TL (bottom smooth traces, $I_l + I_r$) data obtained for 10 mM $Eu(dpa)_3^{3-}$ in D_2O at nine different sample temperatures. Excitation was with left-circularly polarized light at 526.3 nm and emission intensities were measured at 594.8 nm. All the TL decay curves are overlaid, whereas the CPL decay curves are offset from one another by 3000 counts on the CPL axis.

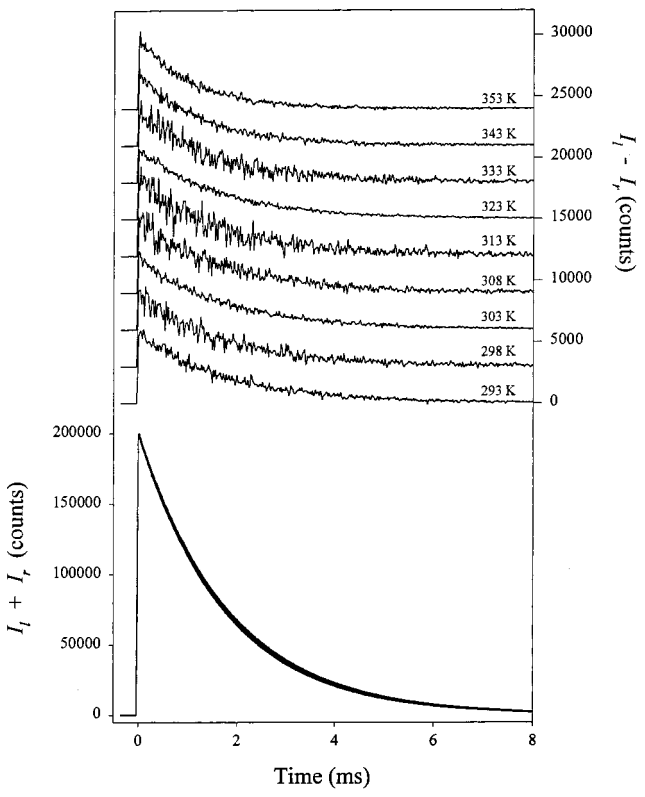

Figure 5. Time-resolved CPL (top noisy traces, $I_l - I_r$) and TL (bottom smooth traces, $I_l + I_r$) data obtained for 10 mM $Eu(dpa)_3^{3-}$ in H_2O−EG (60%) at nine different sample temperatures. Excitation was with left-circularly polarized light at 526.3 nm and emission intensities were measured at 594.8 nm. All the TL decay curves are overlaid, whereas the CPL decay curves are offset from one another by 3000 counts on the CPL axis.

available for following $\Lambda^* \rightleftharpoons \Delta^*$ processes in this system are narrower than those available for $Eu(dpa)_3^{3-}$, and consequently the values of k_c obtained from fits of the $Eu(pe\text{-}dpa)_3^{3-}$ data have larger uncertainties than the values of k_c obtained from fits of $Eu(dpa)_3^{3-}$ data. In Figure 7 we show an Arrhenius plot of the k_c results (with uncertainty bars included) obtained for $Eu(pe\text{-}dpa)_3^{3-}$ in H_2O, over the 303−353 K temperature range.

$Eu(dpa)_3^{3-}$ in CH_3OH, C_2H_5OH, and CH_3CN Solutions. In all of the H_2O, D_2O, and H_2O−EG solution samples examined in this study, the charge-balance cations present in solution with $Eu(dpa)_3^{3-}$ or $Eu(pe\text{-}dpa)_3^{3-}$ were sodium ions. However, in each of the CH_3OH, C_2H_5OH, and CH_3CN solution samples examined, the charge-balance cations were tetra-*n*-butylammonium (NBu_4^+) ions introduced in the preparation of these samples from the $(NBu_4)_3[Eu(dpa)_3]$ salt. Conductometric measurements indicate significant cation−anion pairing in the nonaqueous solution samples of $(NBu_4)_3[Eu(dpa)_3]$.[8] This ion-pairing has essentially no discernible effects on the optical excitation and emission spectra of the $Eu(dpa)_3^{3-}$ complexes, but one would expect it to have significant retardation effects on $\Lambda^* \rightleftharpoons \Delta^*$ enantiomer interconversion kinetics. In agreement with this expectation, the CPEx/TR-CL experiments performed on $Eu(dpa)_3^{3-}$ in CH_3OH, C_2H_5OH, and CH_3CN solutions show no evidence of $\Lambda^* \rightleftharpoons \Delta^*$ processes occurring over time periods as long as 6 ms, at temperatures up to 40−60 °C. The luminescence decay constants (k_0) measured for $Eu(dpa)_3^{3-}$ in CH_3CN range from 380 s^{-1} (at −20 °C) to 361 s^{-1} (at 60 °C), and they are of similar magnitude (but ca. 10% larger) for $Eu(dpa)_3^{3-}$ in CH_3OH and C_2H_5OH. These k_0 values are somewhat smaller than those observed for the H_2O solution samples but are larger than those observed for the D_2O solution samples.

(8) Hopkins, T. A. Unpublished results.

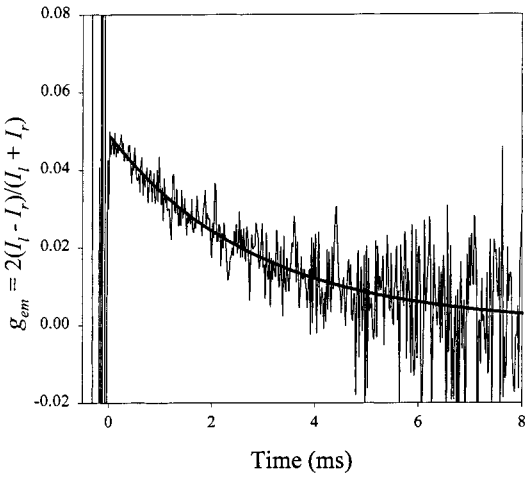

Figure 6. Time-resolved emission dissymmetry factor data obtained for 10 mM $Eu(dpa)_3^{3-}$ in H_2O−EG (60%) at 353 K. Excitation was with left-circularly polarized light at 526.3 nm and emission intensities were measured at 594.8 nm. The heavy smooth line through the data is the best-fit exponential decay obtained by fitting the experimental data to eq 19 of the text.

Discussion

The trisdipicolinate coordination complexes of europium(III) and terbium(III) have been used in a number of recent studies

Table 1. Rate Constants (in s^{-1}) Determined from CPEx/TR-CL Measurements on $Eu(dpa)_3^{3-}$ Complexes in H_2O, D_2O, and H_2O-EG Solution Samples

	H_2O		D_2O		H_2O-EG	
T (K)	k_0	k_c[a]	k_0	k_c[a]	k_0	k_c[a]
353	641	592(35)	329	370(57)	568	174(7)
343	637	338(23)	327	299(23)	559	94(5)
333	633	197(12)	326	161(9)	552	47(7)
323	629	114(4)	325	100(7)	546	25(2)
313	627	70(7)	323	42(5)	545	n.d.
308	625	42(4)	322	48(12)	543	15(5)
303	623	32(2)	321	30(6)	538	6(2)
298	621	24(5)	319	17(4)	535	9(4)
293	619	12(7)	318	6(3)	533	8(3)
288	613	n.d.	318	n.d.	532	n.d.
283	612	n.d.	317	n.d.	531	n.d.
278	610	n.d.	315	n.d.	529	n.d.
273	608	n.d.	314	n.d.	526	n.d.
268					524	n.d.
263					521	n.d.
258					518	n.d.
253					516	n.d.

[a] Numbers shown in parentheses correspond to uncertainties in the values of k_c derived from fits of $g_{em}(\lambda',t)$ data to eq 19; n.d. ≡ not determined.

Table 2. Thermal Activation Parameters Determined for $\Lambda^* \rightleftharpoons \Delta^*$ Enantiomer Interconversion Kinetics of $Eu(dpa)_3^{3-}$ and $Eu(pe\text{-}dpa)_3^{3-}$ Complexes in Solution

	$Eu(dpa)_3^{3-}$			$Eu(pe\text{-}dpa)_3^{3-}$
parameter	H_2O	D_2O	H_2O-EG	H_2O
Arrhenius[a]				
E_a (kJ/mol)	51.3(1.3)	50.7(2.4)	56.1(2.1)	69.9(6.3)
ln A (s^{-1})	23.8(0.5)	23.4(0.9)	24.2(0.7)	30.9(2.3)
Eyring[b]				
$\Delta H^{\ddagger}$ (kJ/mol)	48.6(1.3)	48.0(2.4)	53.3(2.1)	67.2(6.3)
$\Delta S^{\ddagger}$ (J/mol K)	−55.8(3.9)	−59.3(7.3)	−52.7(6.1)	3(20)

[a] Arrhenius parameters determined from fits of $k_c(T)$ data to $\ln k_c = \ln A - E_a/RT$. [b] Eyring parameters determined from fits of $k_c(T)$ data to $\ln(k_c/T) = \ln(k_B/h) + \Delta S^{\ddagger}/R - \Delta H^{\ddagger}/RT$.

Table 3. Rate Constants Determined from CPEx/TR-CL Measurements on $Eu(pe\text{-}dpa)_3^{3-}$ Complexes in H_2O Solution Samples

T (K)	k_0 (s^{-1})	k_c (s^{-1})[a]
353	1254	1120(110)
343	1179	550(30)
333	1109	260(50)
323	1043	220(40)
313	992	43(16)
303	936	22(15)
293	907	4(8)

[a] Numbers shown in parentheses correspond to uncertainties in the values of k_c derived from fits of $g_{em}(\lambda',t)$ data to eq 19.

as luminescent probes of intermolecular chiral recognition processes in solution.[4,9−19] In these studies, the $Ln(dpa)_3^{3-}$ complexes (where Ln ≡ Eu^{3+} or Tb^{3+}) are present in solution with a resolved or partially resolved concentration of optically active (chiral) molecules that can act as quenchers of $Ln(dpa)_3^{3-}$ luminescence. The $Ln(dpa)_3^{3-}$ complexes in the solution samples are excited with a pulse of racemic (unpolarized or linearly polarized) light to produce a racemic excited-state population of Λ* and Δ* enantiomers, and the differential decay kinetics of the Λ* and Δ* subpopulations are monitored by TR-CL measurements. Any differences observed in the decay kinetics of the Λ* and Δ* sub-populations may be ascribed to differential Λ*-CQ vs Δ*-CQ quenching interactions and rate processes (where CQ denotes a chiral quencher molecule), and the rate constants determined from the TR-CL measurements give information about both the degree and sense of the chiral recognition (or discrimination) that occurs in the quenching processes. In these experiments, the time evolution of enantiomeric excess in the emitting-state population of luminophores is given by[3,4]

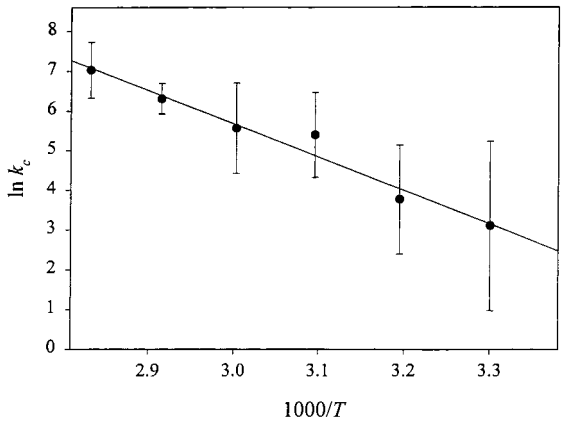

Figure 7. An Arrhenius plot of the enantiomer interconversion rate constants (k_c) determined for $Eu(pe\text{-}dpa)_3^{3-}$ in H_2O solution over the 303−353 K temperature range.

$$\eta_{em}(t) = \frac{2k_q E_q [CQ]\tanh(Zt/2)}{Z + 2k_c \tanh(Zt/2)} \qquad (22)$$

where [CQ] denotes quencher concentration in the solution sample, tanh denotes a hyperbolic tangent function, k_c is the rate constant for $\Lambda^* \rightleftharpoons \Delta^*$ enantiomer interconversion processes, and the k_q, E_q, and Z parameters are defined by $k_q = (k_q^{\Delta^*} + k_q^{\Lambda^*})/2$, $E_q = (k_q^{\Delta^*} - k_q^{\Lambda^*})/(k_q^{\Delta^*} + k_q^{\Lambda^*})$, and $Z = 2[(k_q E_q[CQ])^2 + k_c^2]^{1/2}$, where the $k_q^{\Delta^*}$ and $k_q^{\Lambda^*}$ parameters are the rate constants for Δ*-CQ and Λ*-CQ bimolecular quenching processes.

The expression given above for $\eta_{em}(t)$ reflects a competition between the kinetics of enantiopreferential quenching processes, which *create* enantiomeric excess in the emitting-state population of luminophores, and the kinetics of $\Lambda^* \rightleftharpoons \Delta^*$ processes, which act to *diminish* this enantiomeric excess. Under conditions in which $2k_c \ll |k_q^{\Delta^*} - k_q^{\Lambda^*}|[CQ]$, the $\Lambda^* \rightleftharpoons \Delta^*$ processes are too slow to affect $\eta_{em}(t)$ within the time periods of TR-CL data collection, and they may be ignored in detailed analyses

(9) Metcalf, D. H.; Snyder, S. W.; Demas, J. N.; Richardson, F. S. *J. Am. Chem. Soc.* **1990**, *112*, 5681−5695.
(10) Richardson, F. S.; Metcalf, D. H.; Glover, D. P. *J. Phys. Chem.* **1991**, *95*, 6249−6259.
(11) Metcalf, D. H.; Stewart, J. M. M.; Snyder, S. W.; Grisham, C. M.; Richardson, F. S. *Inorg. Chem.* **1992**, *31*, 2445−2455.
(12) Rexwinkel, R. B.; Meskers, S. C. J.; Riehl, J. P.; Dekkers, H. P. J. M. *J. Phys. Chem.* **1992**, *96*, 1112−1120.
(13) Rexwinkel, R. B.; Meskers, S. C. J.; Dekkers, H. P. J. M.; Riehl, J. P. *J. Phys. Chem.* **1992**, *96*, 5725−5733.
(14) Rexwinkel, R. B.; Meskers, S. C. J.; Riehl, J. P.; Dekkers, H. P. J. M. *J. Phys. Chem.* **1993**, *97*, 3875−3884.
(15) Rexwinkel, R. B.; Meskers, S. C. J.; Dekkers, H. P. J. M.; Riehl, J. P. *J. Phys. Chem.* **1993**, *97*, 13519−13526.
(16) Metcalf, D. H.; Bolender, J. P.; Driver, M. S.; Richardson, F. S. *J. Phys. Chem.* **1993**, *97*, 553−564.
(17) Bolender, J. P.; Metcalf, D. H.; Richardson, F. S. *Chem. Phys. Lett.* **1993**, *213*, 131−138.
(18) Maupin, C. L.; Meskers, S. C. J.; Dekkers, H. P. J. M.; Riehl, J. P. *Chem. Commun.* **1996**, 2457−2458.
(19) Meskers, S. C. J.; Ubbink, M.; Cauters, G. W.; Dekkers, H. P. J. M. *J. Phys. Chem.* **1996**, *100*, 17957−17971.

of the TR-CL data. However, when these conditions are not met, the rate parameters obtained from the data analyses include contributions from k_c, and these contributions must be accounted for to obtain values for the rate parameters that govern the enantiopreferential quenching kinetics (i.e., $k_q^{\Lambda^*}$, $k_q^{\Delta^*}$, and/or k_qE_q).

Most of the enantiopreferential quenching studies reported to date have been carried out on H_2O, D_2O, H_2O-EG, or methanol solution samples that contained a 1−10 mM concentration of either $Eu(dpa)_3^{3-}$ or $Tb(dpa)_3^{3-}$ and a 1−100 μM concentration of chiral quencher species. Over the ranges of sample temperatures represented in these studies, the values of $|k_q^{\Delta^*} - k_q^{\Lambda^*}|[CQ]$ (or equivalently, $2k_q|E_q|[CQ]$) were determined to generally fall within the 10−1000 s^{-1} range, with the lower values being observed at the lower sample temperatures and the higher values being observed at the higher temperatures. In essentially all cases *except* where methanol was the solvent, these values of $|k_q^{\Delta^*} - k_q^{\Lambda^*}|[CQ]$ were observed to be less than an order of magnitude larger than the k_c rate constants determined for Λ-$Eu(dpa)_3^{3-} \rightleftharpoons \Delta$-$Eu(dpa)_3^{3-}$ processes at temperatures above 300 K. Therefore, one must take into account the competitive kinetics of enantiomer resolution processes (effected by enantiopreferential quenching) and enantiomer racemization processes (effected by $\Lambda^* \rightleftharpoons \Delta^*$ interconversions). Under these conditions, the *maximum* resolution that can be achieved in the emitting-state population of luminophores is given by

$$\lim_{t\to\infty} |\eta_{em}(t)| = \frac{k_{res}}{(k_{res}^2 + k_{rac}^2)^{1/2} + k_{rac}} \qquad (23)$$

where $k_{res} = |k_q^{\Delta^*} - k_q^{\Lambda^*}|[CQ]$ and $k_{rac} = 2k_c$. Under these same conditions of competitive enantiomer resolution and racemization kinetics, but with a sample excited with a *continuous* (rather than pulsed) light source, the *steady-state* enantiomeric excess achievable in the emitting-state population is given by[3]

$$|\bar{\eta}_{em}| = \frac{k_q|E_q|[CQ]}{k_0 + k_q[CQ] + 2k_c} = \frac{k_{res}/2}{k_0 + k_q[CQ] + k_{rac}} \qquad (24)$$

At any given temperature between 300 and 353 K, the magnitudes of the rate constants determined for Λ-$Eu(dpa)_3^{3-} \rightleftharpoons \Delta$-$Eu(dpa)_3^{3-}$ processes in H_2O, D_2O, and H_2O-EG solutions are observed to fall in the order $k_c(H_2O) > k_c(D_2O) > k_c(H_2O-EG)$. The Arrhenius activation energies determined for these processes fall in the order $E_a(H_2O-EG) > E_a(H_2O) \approx E_a(D_2O)$. The relatively slower kinetics and higher activation energy observed for these processes in H_2O-EG solutions can most likely be attributed to the higher viscosity of the H_2O-EG solvent mixture, compared to that of H_2O and D_2O. Recall from our earlier discussions that the concerted ligand rotational motions involved in the $\Lambda^* \rightleftharpoons \Delta^*$ structural transformations would require significant expansion and/or structural alteration of the solvent cavity about an $Eu(dpa)_3^{3-}$ complex, and the energy requirements for any such changes in local solvent structure would be expected to exhibit a dependence on solvent viscosity. The differences observed between the kinetics of $\Lambda^* \rightleftharpoons \Delta^*$ processes in H_2O and D_2O solutions are most likely due to mass effects on the rotational motions of ligands coupled strongly to solvent molecules (via *specific* H-bonding or D-bonding interactions at the carboxylate groups of the dpa ligands).

Throughout our discussions of $\Lambda^* \rightleftharpoons \Delta^*$ processes in this paper, we have assumed that these processes occur via *intramolecular* structural transformations that involve no entry of solvent molecules into the inner-coordination sphere of the metal ion. It is assumed throughout that ligand(dpa)-solvent exchange and bound ligand-free ligand exchange processes are too slow to make significant contributions to the observed enantiomer interconversion kinetics. The results obtained from our spectroscopic measurements cannot provide *conclusive* proof that these assumptions are valid, but they do indicate that the only emitting species with detectable concentrations in the sample solutions are structurally intact Λ^* and Δ^* isomers of the metal complexes. The time-resolved $I(\lambda',t)$, $\Delta I(\lambda',t)$, and $g_{em}(\lambda',t)$ measurements yield data that show the *single-exponential* decay behavior predicted by eqs 13−15, and the $I(\lambda')$ and $\Delta I(\lambda')$ intensity spectra show spectral dispersion properties diagnostic of intact, trigonally symmetric $Eu(dpa)_3^{3-}$ luminophores. These observations do not prove the absence of other structural species in the solution samples, but if these other species exist, they are either very short-lived or are present in very low concentrations.

Detailed descriptions of intramolecular $\Lambda \rightleftharpoons \Delta$ isomerization processes in chiral, tris-chelated metal complexes generally focus on two alternative structural-transformation mechanisms, which are commonly referred to as the *trigonal-twist* (or Bailar) mechanism and the *rhombic-twist* (or Ray−Dutt) mechanism.[20,21] Applied to intramolecular $\Lambda \rightleftharpoons \Delta$ structural transformations of $Eu(dpa)_3^{3-}$, the trigonal-twist mechanism would involve a *concerted* twist (or partial rotation) of all three bicyclic chelate rings about their respective C_2 axes, following a path that conserves the C_3 symmetry axis of the complex and carries the complex through a transition-state structure of D_{3h} point-group symmetry. The rhombic-twist mechanism, on the other hand, would involve the twisting of just two chelate rings (as a unit) about the C_2 axis of the third chelate ring in the complex, and it would carry the complex through a transition-state structure of C_{2v} point-group symmetry. Figure 8 of ref 1 shows structural representations of the transition-state species predicted to be formed along the two mechanistic pathways. Our experiments provide no clues regarding which pathway might be favored, and molecular mechanics calculations on weakly coordinated metal complexes are not sufficiently reliable to give useful information. Furthermore, the strong solvent dependence exhibited by our enantiomer interconversion rate data indicates that any detailed consideration of mechanism must include explicit consideration of solvation energetics and local solvent structure.

Acknowledgment. This work was supported in part by a research grant from the U.S. National Science Foundation (to F.S.R.) and by a research fellowship award (to V.J.P.) from the University of Virginia Burger−Lutz Graduate Fellowship Endowment.

IC9713700

(20) Minor, S. S.; Everett, G. W., Jr. *Inorg. Chem.* **1976**, *15*, 1526−1530.
(21) Rodger, A.; Johnson, B. F. G. *Inorg. Chem.* **1988**, *27*, 3061−3062.